



Contents lists available at ScienceDirect

Quaternary International

journal homepage: www.elsevier.com/locate/quaint

Simulation of hydrological processes and effects of engineering projects on the Karkheh River Basin and its wetland using SWAT2009

Yasser Ghobadi ^a, Biswajeet Pradhan ^{a, *}, Gholam Abbas Sayyad ^b, Keivan Kabiri ^c,
Yashar Falamarzi ^d

^a Department of Civil Engineering, Geospatial Information Science Research Center (GISRC), Faculty of Engineering, University Putra Malaysia, 43400, Serdang, Selangor, Malaysia

^b Department of Soil Science, Faculty of Agriculture, Shahid Chamran University of Ahwaz, Ahwaz, Iran

^c Department of Satellite Oceanography, Iranian National Institute for Oceanography and Atmospheric Science, Tehran, Iran

^d Agricultural and Biological Engineering Department, Faculty of Engineering, University Putra Malaysia, 43400, Serdang, Selangor, Malaysia

ARTICLE INFO

Article history:

Available online xxx

Keywords:

Simulation
SWAT model
SUF2
Uncertainty analysis
Engineering projects
KRB

ABSTRACT

Limited water supply is one of the major restrictions in development and agricultural activities in numerous countries, especially in arid and semi-arid regions. Wetlands are constantly affected by anthropogenic factors such as engineering projects and landscaping. Therefore, simulation of hydrologic processes and modeling the factors involved are important. In this study, Soil and Water Assessment Tool (SWAT) was used to simulate the hydrologic process in the Karkheh River Basin (KRB) in southwest Iran and to evaluate the impacts of engineering projects on its wetland (Al Hawizeh) located in the Iran–Iraq border. Calibration, validation, and uncertainty analysis were performed using Sequential Uncertainty Fitting Ver. 2 (SUFI2), which is one of the program interfaces with SWAT, in the Package SWAT Calibration Uncertainty Programs (SWAT-CUP). To assess the goodness of calibration and validation, four measures were applied: (i) percentage of data bracketed by 95% prediction uncertainty or *P*-factor (95PPU) calculated at 2.5% and 97.5% intervals of the simulated variables, (ii) *R*-factor, which is the ratio of average thickness of the PPU, (iii) Nash–Sutcliffe coefficient (NSE), and (iv) determination of coefficient (R^2). Stream flows from four gauge stations combined with 14 synoptic stations were used for calibration (1987–1990) and validation (1991–1994). The *P*-factor values for these stations ranged from 0.64 to 0.84 and from 0.65 to 0.79 for calibration and validation, respectively. These results showed reasonable accuracy according to literature. NSE values were also acceptable, ranging from 0.52 to 0.8 and from 0.62 to 0.72 for calibration and validation, respectively. R^2 values were also within an acceptable range. The calibration and validation results were then used to simulate two watershed scenarios (with and without a dam). In addition, annual flow volumes (AFVs) for two downstream stations (Hamidiyeh and Pay e Pol) were computed. AFV is defined as the volume of water that discharges from catchment at the desired output during a year. The results showed that the flows during 1987–2000 (before dam construction) and 2001 to 2010 (after dam construction) were significantly reduced after the Karkheh dam construction. The corresponding AFVs for the Hamidiyeh and Pay e Pol stations were 8.92×10^{11} and $1.04 \times 10^{12} \text{ m}^3$ in 1987–2000 and 2.57×10^{11} to $3.94 \times 10^{11} \text{ m}^3$ in 2001–2010. Thus, the AFVs before and after dam construction were reduced to 6.34×10^{11} and $6.53 \times 10^{11} \text{ m}^3$ for the Hamidiyeh and Pay e Pol gauges, respectively. Consequently, flow reduction affected the wetland area, in which the surface area of the wetland was reduced and dust emission was increased.

© 2015 Elsevier Ltd and INQUA. All rights reserved.

1. Introduction

Water is the most critical global resource and also the most misused one. It is essential for agriculture, industrial, domestic, and municipal activities (Masih et al., 2009). Governments across the globe have adopted various measures to address the changing

* Corresponding author.

E-mail address: biswajeet24@gmail.com (B. Pradhan).

lifestyle and population growth. Agricultural production has been increased to satisfy the increasing demands of people (Jones et al., 2008). Many arid and semi-arid countries have adopted various aggressive approaches toward agriculture without properly analyzing the environmental and hydrological effects of their projects. For instance, dust storms have been one of the most significant environmental concerns during the last decade and in the Middle East. Agricultural projects that addressed this concern in arid and semi-arid regions have reduced the natural water availability, thereby damaging aquatic ecosystems (Ahmad et al., 2009).

Iran has vast land resources but has scarce water resources, which exemplifies these challenges. This region is dry and characterized by below 0.4% of the global level fresh water (Dinpashoh et al., 2004). Karun, Dez, and Karkheh are three largest rivers among the many rivers in Iran. Many rivers and streams flow through steep and irregular landscapes, thus these conditions end up in marshes and wetlands. Large-scale wetland and marshes throughout Iran are essential in terms of their biodiversity as well as environmental and socio-economic values. The majority of these water resources (~93%) is utilized for agriculture (Ahmad et al., 2009). The Karkheh River Basin (KRB) is one of the most productive watershed area in Iran, and it involves ~9% of total irrigated area in the country (Marjanizadeh et al., 2009). The water availability and consumption in the KRB was assessed between 2002 and 2003, and results indicated that KRB is a scarce water resource (Muthuwatta et al., 2010). Hydrology is a main component that impacts wetland systems, and biogeochemical cycles are influenced by hydrological processes. Hydrology controls the structure and functions of wetland ecosystems as well as impacts soil salinity, microbial activity, and nutrient availability (Feng et al., 2013). The KRB and Al Hawizeh wetland have undergone numerous alterations because of aggressive water management projects by Iran and its neighbors in southwest Iran. The wetland that extended over an area of ~3386 km² in 1985 declined to ~925 km² in 2002 (Ghobadi et al., 2015). Land use and land cover (LULC) changes occurred over the Al Hawizeh wetland and KRB. This condition reflects the effect of huge engineering projects in Syria, Turkey, Iraq, and Iran. According to studies by Jones et al. (2008) the storage capacities of the dams in these countries are as follows: Tabaqa dam, 11.7 × 10⁹ m³; Tishirine dam, 1.9 × 10⁹ m³; Atatürk dam, 48.7 × 10⁹ m³; Keban dam, 31 × 10⁹ m³; and Karkheh dam, 7.8 × 10⁹ m³. The Karkheh dam (operation and filled in 2001), had long been mooted to irrigate large plain tracts, to generate hydro-power, and to provide high quality drinking water (Marjanizadeh et al., 2009).

Proper planning for the use and protection of water resource, as well as evaluation of the changes in environmental conditions, requires basin runoff models that can simulate flow regimes (Mango et al., 2011). The Soil and Water Assessment Tool (SWAT) model is an open source code that provides users with flexibility for performing required modifications, such as in continuous model and geographic information system (GIS) data sets that were created for the watershed and could be easily imported to the model, and then applied in various investigations (Abbaspour et al., 2007b; Jones et al., 2008). Several studies have been carried out by the SWAT model. This model was applied in Lake Tana Basin in Ethiopia to simulate the hydrologic and impact of climate change (Setegn et al., 2010, 2011). In another study, Abbaspour et al. (2007b), simulated the Thur watershed using SWAT model and calibrated by SUFI-2 algorithm involving all related process affecting water quantity, sediment, and nutrient load. Similarly, Tana River Basin and its reservoir, Masinga, was assessed by the SWAT model to predict impacts of landuse (Jacobs et al., 2007). Yan et al. (2013) applied an integrated approach involving hydrological modelling (SWAT) and partial least squares regression (PLSR) to

quantify the contributions of changes in individual land use types in streamflow and sediment yield. Yang et al. (2008) compared five uncertainty analysis procedures such as: Generalized Likelihood Uncertainty Estimation (GLUE), Parameter Solution (ParaSol), Sequential Uncertainty Flattening algorithm (SUFI-2), Markov Chain Monte Carlo (MCMC), and Importance Sampling (IS) techniques. The SWAT model was used to evaluate and model the runoff in the Sondu river basin in Kenya (Jayakrishnan et al., 2005). Arnold et al. (2010) employed Soil and Water Assessment Tool (SWAT) watershed model to simulate water flow across discretized landscape units. SWAT 2005 was applied to compare the impacts of different climate datasets (station and gridded) for the Xiangxi River by simulating discharge (Xu et al., 2010). ArcView-SWAT (AVSWAT) 2000 model was applied to Gucheng Lake, which is a small catchment that is located in the Yangtze River basin. This application simulated water discharge and pollutant loading during 1951–2000 (Huang et al., 2009). Liu et al. (2011) investigated impacts of climate change on streamflow in the Yellow River Basin using semi distributed hydrological model (SWAT) during 1961–2009. In a separate study, the model was applied to the Xiangchi catchment in China to parameterize the SWAT model (Hörmann et al., 2009). Santhi et al. (2006), applied this model to performed extensive stream flow validation for two Texas watersheds that cover over 4000 km². Kim et al. (2010), compared flow and loads from SWAT2005 using the Muskingum method of stream routing, with a version of SWAT adopted to include a new nonlinear storage routing method. Several studies on the stream flow and surface runoff have also been reported (Chu and Shirmohammadi, 2004; Cao et al., 2006; Arnold et al., 2010; Srinivasan et al., 2010; Bannwarth et al., 2014; Khoi and Suetsugi, 2014). In addition, the impacts of climate change on water and nitrogen cycles in arid central Arizona were evaluated by investigating the second-generation coupled global climate model (CGCM2) and SWAT (Ye and Grimm, 2013). Xu et al. (2009) simulated the corresponding future streamflow regime in the headwater catchment of the Yellow River basin. Three benchmark periods were simulated for the period 2010–2039 (2020s), 2040–2069 (2050s) and 2070–2099 (2080s). Kousari et al. (2010) performed the effects of concentration time on watershed area, amount of rainfall at different return periods and the α -coefficient on the nature of the SCS curve using SWAT and MATLAB program. In this study, SWAT was applied to simulate the stream flow in the KRB from 1987 to 2010, and parameterization approach was used based on two scenarios, that is, with or without a dam. SWAT 2009 was applied in the KRB, which is one of the largest watersheds in Iran. Furthermore, SUFI-2 algorithm was applied for calibration, validation, and uncertainty analysis. The hydrologic impacts of engineering projects on the KRB were assessed. In addition, the impacts of this hydrologic process on the wetland area were analyzed, and the relationship between simulated stream flow and wetland area was established. Finally, the effects of engineering project on increasing dust, as well as the role of wetland in decreasing or increasing the dust in the region, were evaluated.

2. Material and methods

2.1. SWAT model overview

Soil and Water Assessment Tool is a basin-scale, semi-distributed, continuous-time, and eco-hydrological model that operates on a daily time setup and is designed to predict discharge, sediment yield, erosion, as well as pesticide and nutrient load under different scenarios of landuse or climate change (Arnold et al., 1998; Neitsch et al., 2005; Gassman et al., 2007). The model is physically based, computationally efficient, and can continuously simulate over long

periods. The major components of the model are weather, hydrology, soil temperature and properties, plants growth, nutrients, pesticides, bacteria and pathogens (Arnold et al., 2011). In SWAT a watershed is divided into multiple sub-basins, which are then further subdivided into hydrologic response units (HRUs) that consist of homogeneous landuse, management, and soil characteristics. This model allows the simulation with of different physical processes in the watershed, including water movement, sediment generation, deposition, and nutrient fate and transport. The hydrologic cycle, as simulated by SWAT, is based on the water balance equation (Shi et al., 2011).

$$SW_t = SW_0 + \sum_{i=1}^t (R_{day} - Q_{surf} - E_a - W_{seep} - Q_{lat} - Q_{gw}) \quad (1)$$

where, SW_t is the final soil water content (mm water), SW_0 is the initial soil water content on day i (mm water), t is the time (days), R_{day} is the amount of precipitation on day i (mm water), Q_{surf} is the amount of surface runoff on day i , (mm H₂O), E_a is the amount evapotranspiration on day i (mm H₂O), W_{seep} is the amount of water entering the vadose zone from the soil profile on day i (mm water), Q_{lat} is the lateral flow from soil to channel and Q_{gw} is amount of return flow on day i (mm water). The foundation behind the hydrologic simulation in SWAT is soil water balance (Neitsch et al., 2005), in which the model tracks precipitation (measured data), and simulated soil water content, surface runoff, evapotranspiration, percolation, and return flow on a daily basis.

A second trend that has paralleled the historical development of SWAT is the creation of various GIS and other interface tools to support the input of topographic, landuse, soil map, stream network, and other digital data into SWAT. The first GIS interface program developed for SWAT was SWAT/GRASS which was built within the GRASS raster-based GIS (Gassman et al., 2007). The ArcView-SWAT (AVSWAT) interface tool (Neitsch et al., 2005) was designed to generate model inputs from ArcView 3.X GIS data layer and execute SWAT2000 within the same framework of SWAT. Automatic sensitivity, calibration and uncertainty analysis can also be initiated with AVSWAT-X for SWAT2005 (Neitsch et al., 2005). A SWAT interface that is compatible with Arc GIS 9.X and 10.X (ArcSWAT) has been used for geodatabase approach and has a programming structure consistent with Component Object Model (COM) protocol. This version of SWAT includes SWAT2009 and SWAT 2012 (Olivera et al., 2006; Seo et al., 2014).

2.2. Description of the study area

The KRB is the third largest watershed in Iran after Karoon and Dez. This Basin is located in south-west Iran and covers an area ~51,000 km². KRB lies between 30° N and 35° N latitude and 46° E to 49° E longitude (Fig. 1). It is one of the most productive river basins in Iran and occupies ~9% of the total irrigated area (0.6 Mha) of the country. In addition, ~80% of the basin area is part of the Zagros mountain ranges where almost all of the basin runoff is generated (Marjanizadeh et al., 2009; Masih et al., 2011). Water in this basin is primarily used for agricultural production, domestic supplies, and fish farming. It is also serves to suit the environment, which indicates that a major concern for the area is the sustainability of Al Hawizeh wetland that is at the Ramsar site located at the Iran–Iraq border. The main river in the study area, Karkheh, originates from the Zagros mountain and after passing through ~900 km eventually terminates in the Hawizeh Wetland, a large transboundary wetland shared with Iraq, which is connected to the Euphrates-Tigris system and afterward fall on the Shat Al-Arab and finally into the Persian Gulf (Fig. 1).

From the hydrological point of view, the KRB is divided into five sub-basins namely, Gamsiab, Qarasou, Kashkan, Seymareh, and South Karkheh. The first four sub-basins are major tributaries to the main stream of Karkheh River whereas the lower Karkheh or south Karkheh is the site of the Karkheh dam (Muthuwatta et al., 2010).

The elevation of the catchment is varies and ranges from less than 10 m above mean sea level (MSL) in the south Karkheh to more than 3600 m in the northern part of the basin. The climate is semi-arid upstream and arid downstream. The amount of precipitation also differs depending on the elevation. Therefore, the southern part of the catchment receives an annual precipitation of ~150 mm, while the northern part reaches up to ~750 mm. The temperature in the upper Karkheh in summertime varies from 23 °C to 36 °C. However, temperature in the lower Karkheh rises to above 40 °C during the same months, which results in high evaporation. By contrast, in wintertime, the mean daily temperature falls to 6 °C and –2 °C in the southern and northern parts, respectively (Ahmad et al., 2009).

2.3. Data input and model setup

Five major input data, which included digital elevation model (DEM), digital stream network, digital land use map, soil map, and climate-related data, were required for each SWAT model setup. Based on the GIS, all digital data were projected and converted to the grid data under the same reference frame.

The DEM in scale of 1:250,000 (Fig. 1) was downloaded from the Aster DEM website (<http://gdem.ersdac.jspacesystems.or.jp/>) and then masked by KRB boundary. The data were used to delineate the watershed borders and extract the stream network. In doing so, Arc Hydro spatial analysis was applied on the DEM, and a natural stream network of the KRB was created by ArcGIS 10.1 (Fig. 1). Digital soil map in scale of 1:250,000 were prepared by Iranian Soil and Water Research Institute (ISWRI). The soil data (Fig. 2a) were used in the simulation analysis, and the data contained soil types and major properties, including percentage of sand, clay, silt, organic matter, organic carbon, bulk density (g cm⁻³), the number and depth of each layer, soil hydrologic group, the USLE factor, and salinity (ds m⁻¹). The existing soil map indicated that the texture of soils varies from fine to medium-texture soil and to rock outcrop (shallow soil). Based on the soil archives of the study area, additional and aforementioned soil parameters of each type of soil and their detail for simulation were defined and inputted into the model. Spatial distribution of landuse map (Fig. 2b) in scale of 1:250,000 were prepared using field data, Landsat TM and ETM+ images, and GIS. A total of, are 11 landuse classes were determined in the KRB, namely: bare soil, farming, forest, marsh, rangeland, salty lands, shrublands, smooth sand surface, urban, water body, and wetland. The four slope categories determined in this study for HRU definition were (a) 0%–25%, (b) 25%–50%, (c) 50%–75%, and (d) >75%.

The climate datasets compiled for SWAT model construction are the following weather data: (a) precipitation, (b) temperature, (c) relative humidity, (d) wind speed, and (e) solar radiation. The first two parameter were compulsory for the model simulation, and the other parameters are optional (Neitsch et al., 2002). In this study, the precipitation, maximum (Max) and minimum (Min) temperatures, and relative humidity were used for model simulation, and the model was extracted from 14 synoptic stations over the study area from 1987 to 2010. For the model input in the climate section, all weather data were used in daily format and the model was run based on daily data. These weather parameters were sourced from the Iran Metrological Organization (IRIMO).

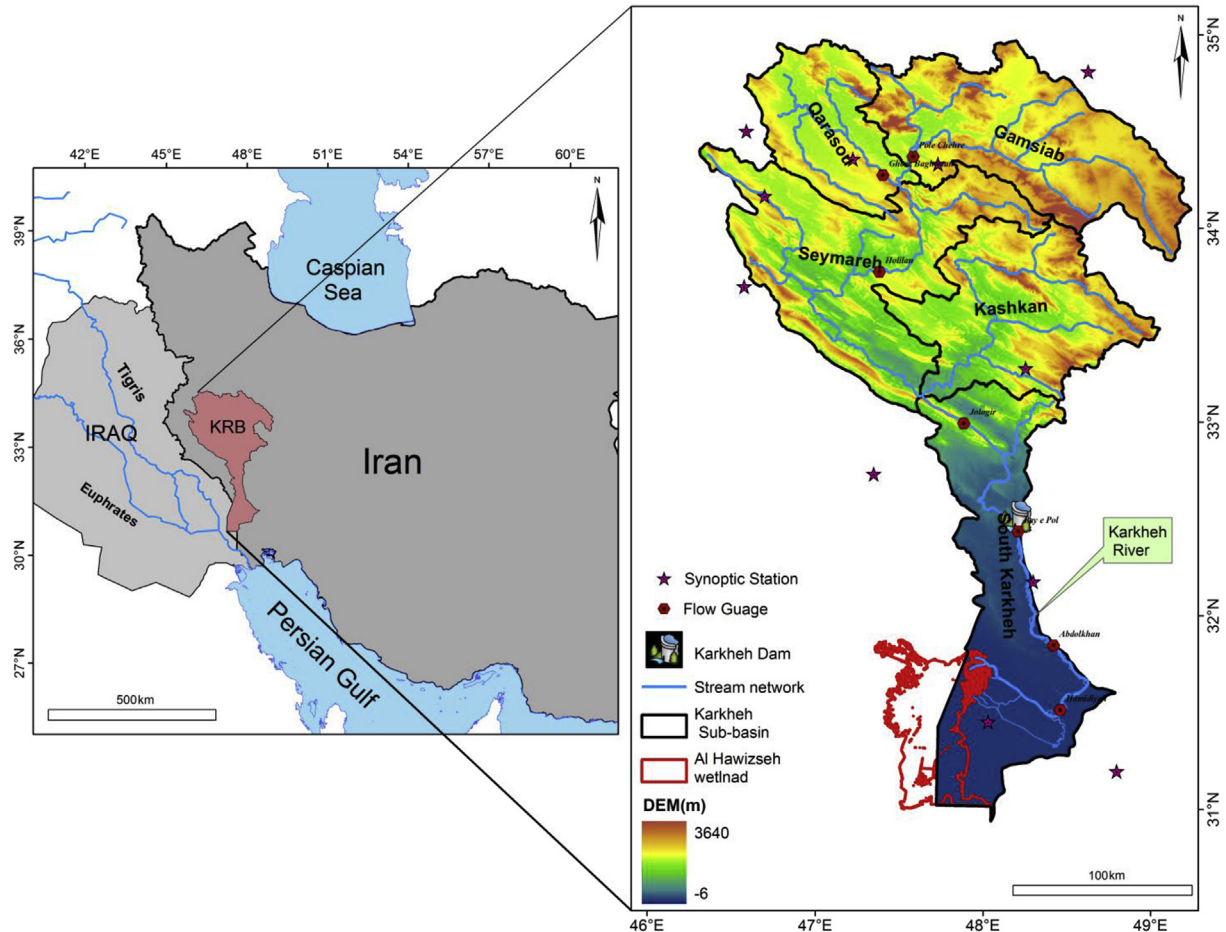


Fig. 1. (a) Location of study area in Iran and (b) the situation of synoptic stations, flow gauges, Karkheh dam, stream flow and al Hawizeh wetland as well as digital elevation model (DEM) of the KRB.

A total of ~50 stream flow gauges were installed over the KRB after 1950. In this study, the monthly data for four stations, namely, Hamidiyeh, Pay e Pol, Ghor Baghestan, and Holilan, were compiled across the study area (Fig. 1 and Table 1). Two of these stations are located upstream (Ghor Baghestan and Holilan), and the rest are situated downstream.

The stations were selected based on geographical importance, availability of consistent length and quality of recorded data. The Pay e Pol station, which is located downstream, is close to the Karkheh dam and an important station for streamflow. It is also the outlet of Holilan and Ghor Baghestan stations and Karkheh dam. The Hamidiyeh River is the last flow station, where it is located before discharge of the Karkheh River into the Al Hawizeh wetland in the Iran–Iraq border. The daily and monthly flow data from 1987 to 2010 and discharge flow of Karkheh dam from 2003 to 2010 were collected from Iran Water Resource Company (IWRC). After the data preparation, SWAT, a physical-based hydrological model, was used to simulate the hydrologic processes and streamflow. Thus, SWAT 2009 (ArcSWAT2009) was used and ran based on different scenarios.

2.4. Sensitivity analysis

A total of 22 hydrological parameters were tested to identify the sensitive parameters for the stream flow simulation using SUFI-2 absolute sensitivity analysis procedure (SUFI-2) (Abbaspour et al., 2004, 2007a; Abbaspour, 2007).

2.5. Model calibration and validation

The model was run for the years 1987–2010 with input that data include DEM, climatic data soil map and parameters, as well as landuse map. The model was calibrated and validated based on observed datasets because of the spatial variability and errors in the input data. Three major sources of uncertainty in output of the watershed model are occurring: i) structural uncertainty, ii) input uncertainty and iii) parameter uncertainty (Abbaspour, 2009). To do this, the study period was divided into a calibration period from 1987 to 1990 and a validation period from 1991 to 1994 for flow on a monthly basis. A model warm-up period of 365 days was used to initialize the model. The calibration and validation results were used to simulate the period from 2003 to 2010 (the period of operation of the Karkheh Dam). The transition period from 1995 to 2002, during which the dam was under construction, was ignored in the analysis. In this study, calibration and uncertainty analysis were implemented using SUFI-2 algorithm available in the soil calibration and uncertainty programs (SWAT-CUP) software to minimize the difference between the observed and predicted flows (Abbaspour, 2009). Latin hypercube sampling is used in SUFI-2 to draw independent parameter sets. In this algorithm, the uncertainty of input parameters were depicted as uniform distributions, whereas model output uncertainty was quantified by 95% prediction uncertainty (95PPU) calculated at the 2.5% and 97.5% level of cumulative distribution of output variables that were obtained through Latin hypercube sampling. SUFI-2 mapped the aggregated

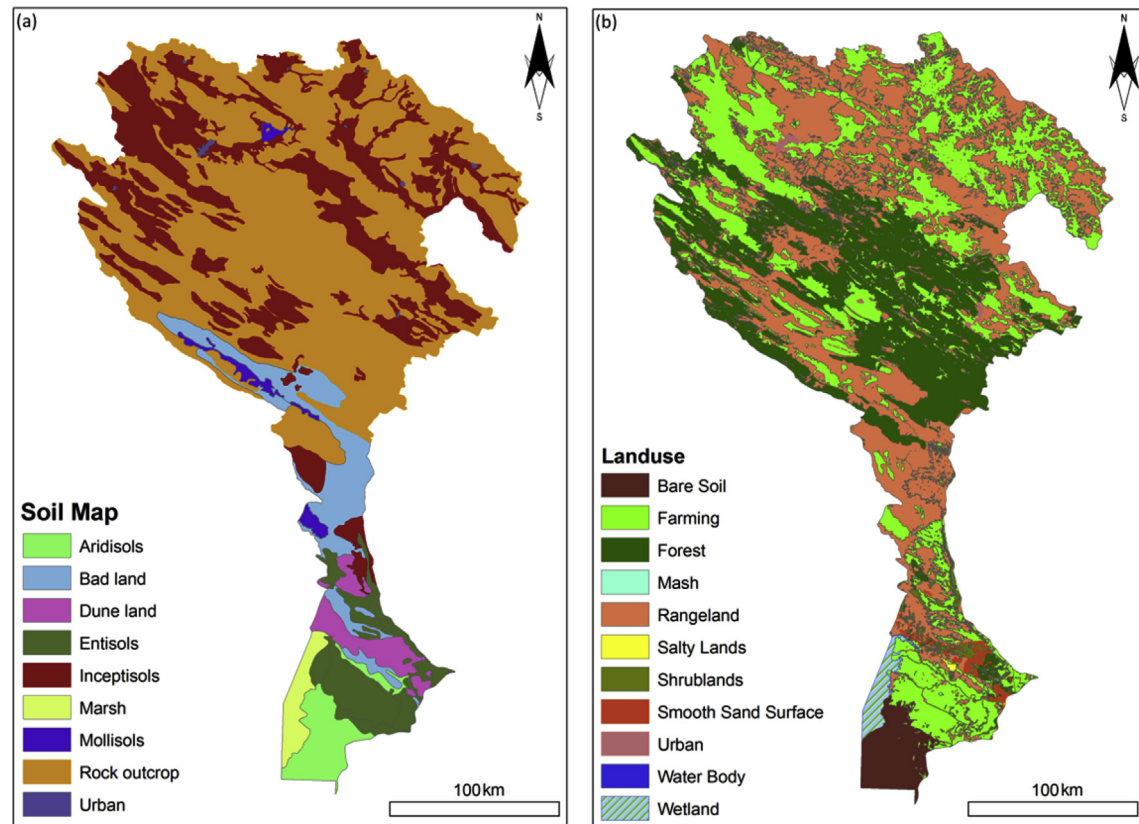


Fig. 2. (a) Distribution of soil type source in the ISWRI, (b) and the distribution of different LULCs derived from Landsat images throughout the KRB.

Table 1

Geographical and hydrological details of the selected streamflow gauging stations in KRB (Masih et al., 2009).

Station name	Sub-basin	Longitude	Latitude	Elevation (msl) ^a	Drainage area (km ²)
Holilan	Seymareh	47.25	33.73	1000	20,863
Gory Baghestan	Qarasou	47.25	34.23	1268	5370
Hamidiyeh	South Karkheh	48.43	31.50	20	46,121
Pay e Pol	South Karkheh	48.15	32.42	125	42,620

^a MSL = mean sea level.

uncertainties to the parameters and obtained the smallest parameter uncertainties (Abbaspour et al., 2007b).

For the accuracy and goodness of fit quantification, different parameters were used: Pearson's correlation coefficient (r), Pearson's coefficient of determination (R^2), percent bias (PBIAS), root mean square error (RMSE), and Nash–Sutcliffe Efficiency coefficient (NSE). This efficiency is commonly used as a quantitative measure of hydrograph prediction performance that helps in the assessment between the predicted and observed flow. NSE is a normalized statistic that determines the relative magnitude of the residual variance (“noise”) compared with the measured data variance (“information”) (Nash and Sutcliffe, 1970). NSE is computed as shown in Eq. (2):

$$NSE = 1 - \frac{\left(\sum_{i=1}^n O_i - P_i \right)^2}{\left(\sum_{i=1}^n O_i - \bar{O} \right)^2} \quad (2)$$

where, NSE is the prediction efficiency, O_i is the observed condition at time i , \bar{O} is the mean of the observed values over all times, and P_i is the predicted value at time i . According to the Moriasi et al. (2007), $NSE > 50$ is acceptable.

Root mean square error (RMSE) observations standard deviation ratio (RSR): RMSE is one of the most commonly used error index statistics (Singh et al., 2005; Moriasi et al., 2007). RSR is calculated as the ratio of the RMSE and standard deviation of measured data, as shown in Eq. (3):

$$RSR = \frac{RMSE}{STDEV_{obs}} = \frac{\left[\sqrt{\sum_{i=1}^n (Q_i^{obs} - Q_i^{sim})^2} \right]}{\left[\sqrt{\sum_{i=1}^n (Q_i^{obs} - Q_i^{mean})^2} \right]} \quad (3)$$

RSR varies from the optimal value of 0, which indicates zero RMSE or residual variation and therefore perfect model simulation, to a large positive value. The lower value of RSR shows the lower value of RMSE and as a result displays a better model simulation.

Pearson's correlation coefficient (r) and coefficient of determination (R^2) describe the degree of co-linearity between simulated and measured data R^2 which describes the proportion of the variance in measured data explained by the model. R^2 ranges from 0 to 1, with higher values indicating less error variance, and typically values greater than 0.5 are considered typically acceptable. The formula for calculating R^2 is shown in Eq. (4).

$$R^2 = \left\{ \frac{\sum_{t=1}^T (Q_{m,t} - \bar{Q}_m)(Q_{s,t} - \bar{Q}_s)}{\left[\sum_{t=1}^T (Q_{m,t} - \bar{Q}_m)^2 \right]^{0.5} \left[\sum_{t=1}^T (Q_{s,t} - \bar{Q}_s)^2 \right]^{0.5}} \right\}^2 \quad (4)$$

where \bar{Q}_m is the mean observed data for the entire evaluation time period, and \bar{Q}_s is the mean simulated data for the entire evaluation period.

In SUFI-2, two different indices were used to compare the measurements of simulation: *P* and *R*-factors. These indices were used to gauge the strength of calibration and uncertainty measures. The *P*-factor is the percentage of measured data bracketed by the 95PPU. The maximum value for *P*-factor is 100% (*P*-factor → 1), and all measured data are ideally included in the 95PPU band. The *R*-factor is calculated as the ratio between the average thickness of the 95PPU band and standard deviation of the measured data. This factor indicates the strength of the calibration and should be close to or smaller than a practical value of 1 (*R*-factor → 0) (Abbaspour et al., 2007b; Schuol et al., 2008). In this study, NSE, *P*-factor, *R*-factor, and R^2 were used to evaluate the goodness of fit.

3. Results and discussion

3.1. Main parameters for calibration

The sensitivity analysis results from the SUFI-2 algorithm are shown in Table 2, which provides the default and best fitted parametric values. These sensitive parameters included: the SCS runoff curve number (II) value (CN2), base flow alpha factor (ALPHA_BF), groundwater delay (GW_DELAY), threshold depth of water in the shallow aquifer required for return flow to occur (GWQMN), Manning's "n" value for overland flow (OV_N), available water capacity of the soil layer (SOL_AWC), soil evaporation compensation factor (ESCO), and average slope length (SLSUBBSN). Consequently, precise estimation of these parameters is important for simulating stream flow in the KRB with SWAT.

3.2. Flow calibration and validation by SUFI-2

Comparative results between the observed and simulation flow discharge values for the calibration and validation periods indicated a good agreement between the observed and simulated flows using SUFI-2 algorithm. Four statistics measures, namely, NSE, R^2 , *P*-factor, and *R*-factor, were used to quantify the achieved calibration levels, and the overall performance of the model was subsequently evaluated. The results of simulated stream flow along the uncertainty band and observed data in the four stations (Ghor Baghestan, Holilan, Pay e Pol, and Hamidiyeh) are presented in Fig. 3.

The calibration [1987–1990 (left)] and validation [1991–1994 (right)] periods show acceptable NSEs (>0.5) for all stations. According to the literature (Santhi et al., 2001; Benaman et al., 2005), a model simulation can be evaluated as satisfactory if R^2 is greater than 0.6. In this case, the results agreed reasonably well with these values (Figs. 3 and 4).

The *P*-factor ranged between 64% and 84% (calibration) and 65% and 79% (validation) whereas *R*-factor ranged from 0.44 to 0.64 (calibration) and 0.47 to 0.99 (validation). There are some poorly simulated stations which showed R^2 values less than 0.5, and small and large *R*-factors, especially for Holilan station during validation. The major reasons for the poor simulation and model calibration are inadequate accounting of agricultural and industrial water use in the model, as well as inter-basin water transfer projects in the humid and arid zones (Faramarzi et al., 2009). In addition, the high uncertainty of stream flow should have been caused by errors in input data such as rainfall and temperature or some channel for agricultural irrigation or other unknown activities in the sub-basin (Setegn et al., 2008). Inspection of the precipitation and temperature data over the KRB showed that this trend is not related to any variation in the precipitation from 1987 to 2010, and climatic differences are not significant to cause the observed general trend of decreasing flow rate by time. In the next step, the effects of engineering projects on the reduced flow throughout the study area are presented.

3.3. Tested scenario result

Two scenarios were determined for the KRB: (1) simulation without a dam (Karkheh), and (2) simulation of stream flow that considered a dam. In this section, the calibration and validation models were used to investigate the impact of dam construction and simulate the flow of the Karkheh River inside the KRB. The simulation inflows were computed for two downstream flow gauge stations, Hamidiyeh and Pay e Pol (Fig. 6).

Dam construction significantly affected the flow discharge downstream, especially at the Al Hawizeh wetland for both flow gauge stations (i.e., Hamidiyeh and Pay e Pol; Fig. 5). The simulated flow under these two scenarios was then used to compute the percentage of reduction in the annual flow (Fig. 6). In addition, annual flow volume (AFV) for the downstream flow gauges was calculated (Fig. 7). AFV for the Hamidiyeh flow gauge station was 8.92×10^{11} and $2.57 \times 10^{11} \text{ m}^3$ from 1987 to 2000 (before Karkheh

Table 2
List of SWAT calibration parameters that were fitted and their final calibration values.

Parameter name	Min default value	Max default value	Best fitted value	Definition
CN2	5.27	47.03	30.43	SCS runoff curve number (II) value
ALPHA_BF	0.05	0.53	0.42	Base flow alpha factor
GW_DELAY	0.15	1.95	1.02	Groundwater delay
GWQMN	0.39	1.90	1.25	Threshold depth of water in the shallow aquifer required for return flow to occur
OV_N	0.34	1.73	1.03	Manning's "n" value for overland flow
SOL_AWC	1.24	2.20	1.78	Available water capacity of the soil layer
ESCO	0.56	1.15	0.91	Soil evaporation compensation factor
SLSUBBSN	1.11	2.18	1.76	Average slope length

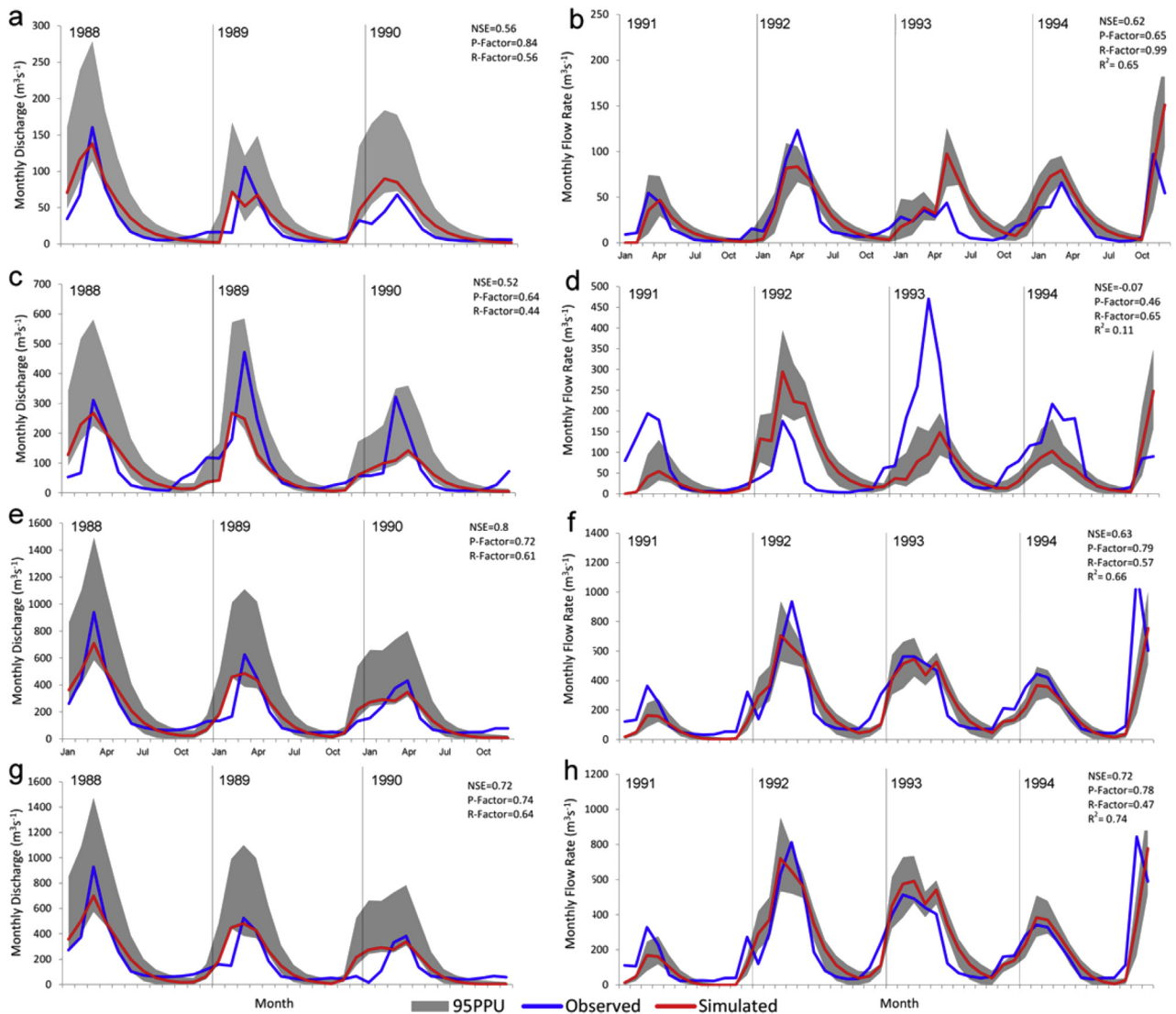


Fig. 3. Calibration (left) and validation (right) results comparing the monthly flow simulation for the Ghor (a–b) Baghestan, (c–d) Holilan, (e–f) Pay e Pol, and (g–h) Hamidiyeh flow gauge stations.

dam construction) and from 2001 to 2010 (after dam construction), respectively. Moreover, the corresponding values for the Pay e Pol flow gauge stations during the same period were 1.04×10^{12} and 3.94×10^{11} m³. Figs. 6 and 7 shows that dam construction reduced the flow discharge to the wetland.

Assessment of the percentage of reduction in AFV from 2003 to 2010 using the simulated and observed flow under the two scenarios illustrates that the amount of reduction ranged from 28% to 100% for Pay e Pol and from 48% to 140% for Hamidiyeh. AFV also slightly decreased for year 2008 in the Pay e Pol station (only 0.05% reduction).

The graph in Fig. 7 shows the moderate reduction in AFV from 1991 to 2000 for both of the flow gauge stations during the construction of the dam, which started to decrease inflow into downstream. The AFV from these two stations evidently reached the lowest value during 2000–2002 because the Karkheh dam started to fill, and increased volume of water became impounded behind the dam or used for other goals, such as irrigation in agricultural field. Therefore, Figs. 6 and 7 demonstrate two ways that by which the dam reduced the flow to the wetland: first is

the impoundment of water behind the Karkheh dam and development of a large artificial lake; the second permanent reduction in flow was by irrigation, infiltration, and evapotranspiration.

The reduction in the flow from Karkheh directly affected the surface area of the Al Hawizeh wetland. Although this wetland is fed by the Tigris River and this river also affected the wetland, only the KRB and Karkheh River flow variation were considered in the current study. By contrast, the huge amount of inflow water into the wetland resulted in the larger area of the wetland and vice versa. The effects of this reduction were investigated, the size of wetland was analyzed, and the areas of wetland before and after dam construction were compared. The analytical and graphical results for 1987 to 2010 showed that in 2002, the lowest inflow water to the wetland was reached when Karkheh dam was impounded and water stored behind it was used for different purposes, such as irrigation and urbanization. In this year, the wetland area was only 925 km² (Ghobadi et al., 2015). This analysis is for the two stations downstream, and the nearest flow gauge station to the wetland is Hamidiyeh, which is located 60 km

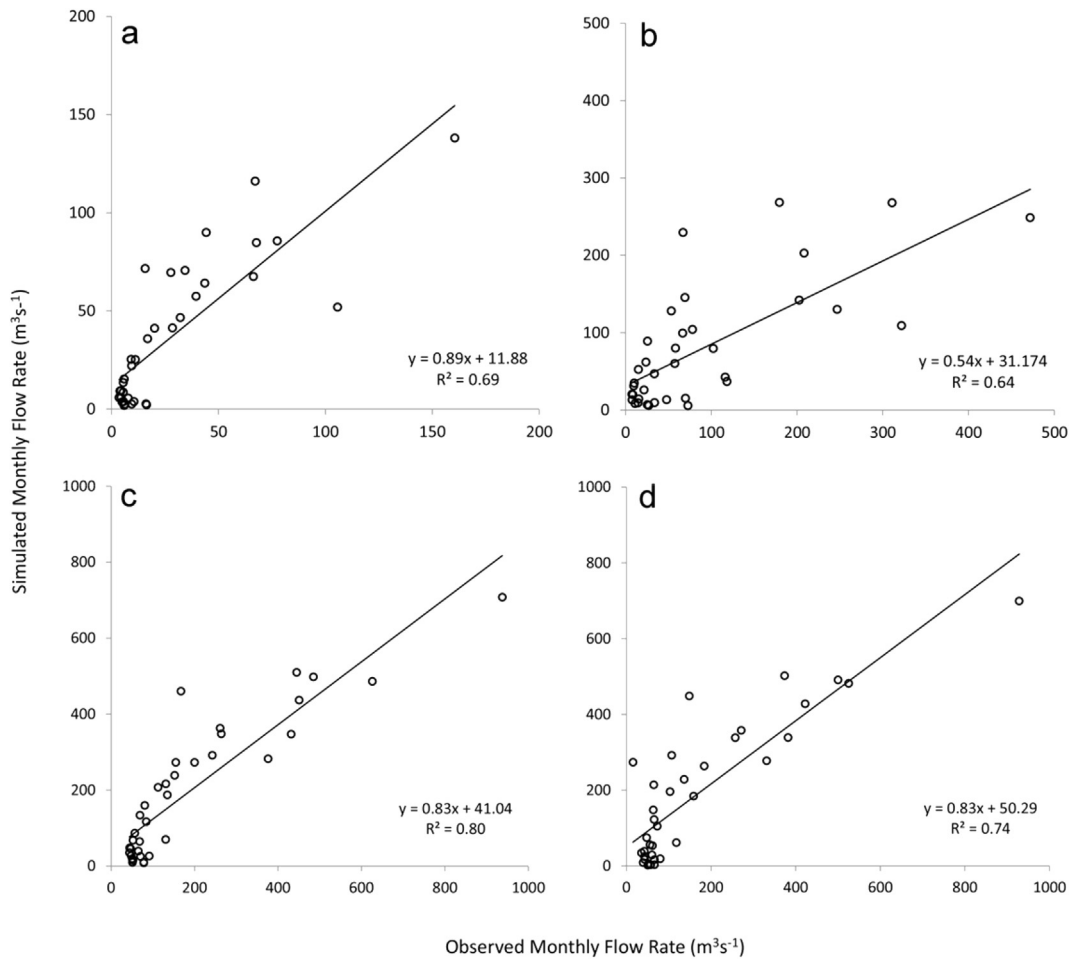


Fig. 4. Observation versus simulation flow rate at the (a) Ghor Baghestan, (b) Holilan, (c) Pay e Pol, and (d) Hamidiyeh during the calibration period (1987–1990).

of Al Hawizeh wetland. Therefore, the loss of flow discharge to the wetland was again reduced considering the agricultural activity around the wetland and also usage of water for the some small city close to the wetland.

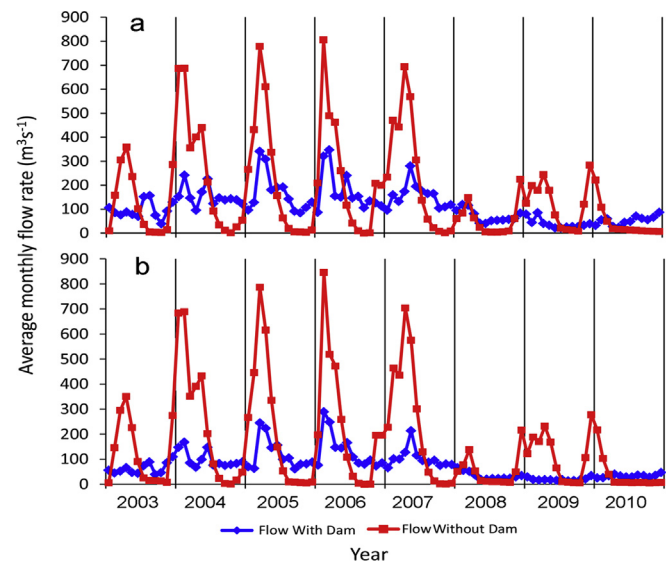


Fig. 5. Simulated monthly flow rate from 2003 to 2010 in the two flow gauge station, (a) Pay e Pol and (b) Hamidiyeh, compared with flow rate that would have existed. This simulation is under two scenarios with dam and without dam.

In the final step, the frequency of dust storm over the study area during 2001 and 2010 was validated. This frequency is also related to inflow reduction and decrease in the wetland area. Based on the data from the Iran Environmental Protection Agency, the frequency of dust storm from 2001 to 2010 increased dramatically. According to these data, the frequency of dust storm in 2001 was only six instances, whereas 36 sandstorms occurred in 2010.

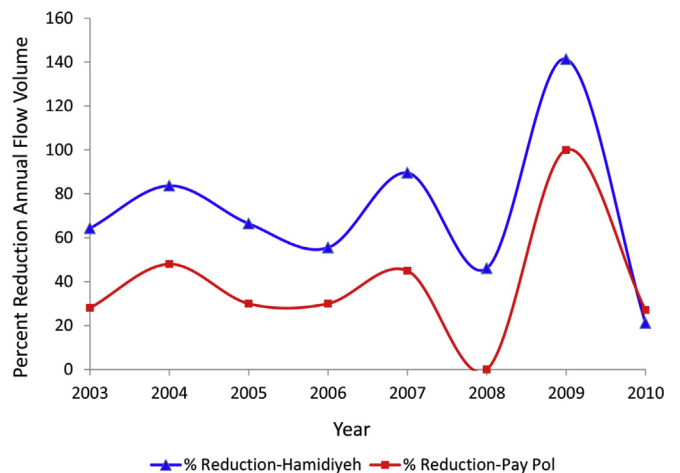


Fig. 6. Percentage of reduction in AFV that resulted from the presence and absence of a dam for period of 2003–2010 in Hamidiyeh and Pay e Pol flow gauge stations.

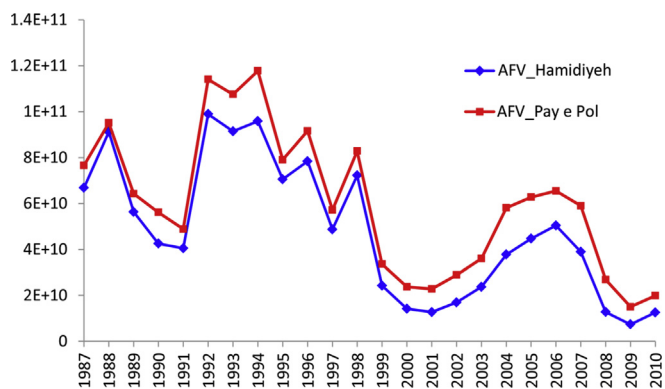


Fig. 7. AFV for Pay e Pol and Hamidiyeh stations from 1987 to 2010.

4. Summary and conclusion

This study simulates the hydrologic impacts of engineering projects in the KRB and its wetland in south-west of Iran during 1987–2010. In doing so, Soil and Water Assessment Tool was used to model the study area and simulate the streamflow throughout the KRB. This model helps in the study of the natural flow system and evaluation the impacts of reduced overall flow into downstream and Al Hawizeh wetland. Five major data inputs for SWAT model were prepared, namely: i) precipitation data, ii) temperature data, iii) relative humidity, iv) soil map of the KRB that was sourced from ISWRI with a scale of 1:250,000 and v) LULC of the basin derived by the different Landsat images which were processed was by ENVI[®] 5.1. A total of 11 landuse classes were determined and prepared for input to the model. DEM was downloaded from the Aster website and the stream network was delineated by the Arc Hydro spatial analysis using ArcGIS10.1[®]. Four flow gauge station were selected for model calibration and validation.

Uncertainty analyses were completed to recognize the sensitive parameters for calibration. Eight sensitive parameters were found, which included CN2, ALPHA_BF, GW_DELAY, GWQMN, OV_N, SOL_AWC, ESCO, and SLSUBBSN. Calibration (1987–1990) and validation (1991–1994) were performed by the SUFI-2 algorithm. The model was successfully calibrated and validated and compared with stream flow data in the KRB with four flow gauge stations. Four statistical parameters were used to evaluate the goodness of fit, namely, *P*-factor, *R*-factor, NSE, and *R*². Based on the literature, all parameters are acceptable (NSE>0.50, *P*-factor>50, *R*-factor <1, and *R*²>60).

The calibration and validation models were used to simulate the AFVs of Karkheh River for two downstream gauge stations, namely, Hamidiyeh and Pay e Pol. The periods with and without a dam were simulated. The AFV for these two stations were for the period from 1987 to 2000 (before dam construction) and 2001 to 2010 (after Karkheh dam construction). Results demonstrated that after dam construction, the AFV decreased dramatically. The AFV results for aforementioned stations were 8.92×10^{11} (1987–2000) and 2.57×10^{11} m³ (2001–2010) (after dam construction) for the Hamidiyeh station. The corresponding values for Pay e Pol for the same period were 1.04×10^{12} and 3.94×10^{11} m³. These results showed that the AFVs for Hamidiyeh and Pay e Pol decreased dramatically compared with the duration before and after Karkheh dam construction (6.34×10^{11} and 6.56×10^{11} m³, respectively). The reduction in flow discharge is directly related to the wetland, considering the inflow into the wetland and wetland area during the period. The high water discharge into the wetland led to an increased wetland area (1987–2000), whereas the reduced inflow to the wetland resulted in

decreased wetland size, especially in 2002. Consequently, the wetland area ultimately decreased, which resulted in the development of a dry area in the region, and increased the incidence of dust storm in the study area either to provide a humid area for filtering the dust aerosol or as a source of dust.

Acknowledgments

The authors gratefully acknowledge Iranian Soil and Water Research Institute (ISWRI), Iran Metrological Organization (IRIMO), and Iran Water Resource Company (IWRC) for the preparation of necessary data sets. Thanks are also Mr. H. Tabatabaei, Eng. Bani Nemeh, and Eng. Torfi for helpful comments. Thanks are due to the two anonymous reviewers for the valuable comments and suggestions that greatly helped to improve this manuscript.

References

- Abbaspour, K., 2007. User Manual for SWAT-CUP. SWAT Calibration and Uncertainty Analysis Programs. Swiss Federal Institute of Aquatic Science and Technology, Eawag, Dübendorf, Switzerland.
- Abbaspour, K., Johnson, C., Van Genuchten, M.T., 2004. Estimating uncertain flow and transport parameters using a sequential uncertainty fitting procedure. *Vadose Zone Journal* 3 (4), 1340–1352.
- Abbaspour, K., Vejdani, M., Haghghat, S., 2007a. SWAT-CUP calibration and uncertainty programs for SWAT. In: MODSIM 2007. International Congress on Modelling and Simulation, Modelling and Simulation Society of Australia and New Zealand, pp. 1596–1602.
- Abbaspour, K.C., 2009. SWAT-CUP2. SWAT Calibration and Uncertainty Programs, Version 2.
- Abbaspour, K.C., Yang, J., Maximov, I., Siber, R., Bogner, K., Mieleitner, J., Zobrist, J., Srinivasan, R., 2007b. Modelling hydrology and water quality in the pre-alpine/alpine Thur watershed using SWAT. *Journal of Hydrology* 333 (2), 413–430.
- Ahmad, M.-U.-D., Islam, M.A., Masih, I., Muthuwatta, L., Karimi, P., Turral, H., 2009. Mapping basin-level water productivity using remote sensing and secondary data in the Karkheh River Basin, Iran. *Water International* 34 (1), 119–133.
- Arnold, J., Allen, P., Volk, M., Williams, J., Bosch, D., 2010. Assessment of different representations of spatial variability on SWAT model performance. *Transactions of the ASABE* 53 (5), 1433–1443.
- Arnold, J., Kiniry, J., Srinivasan, R., Williams, J., Haney, E., Neitsch, S., 2011. Soil and Water Assessment Tool Input/output File Documentation, Version 2009. US Department of Agriculture-Agricultural Research Service, Grassland, Soil and Water Research Laboratory, Temple, TX and Blackland Research and Extension Centre, Texas Agrilife Research, Temple, TX Texas. Water Resources Institute Technical Report(365).
- Arnold, J.G., Srinivasan, R., Muttiah, R.S., Williams, J.R., 1998. Large area hydrologic modeling and assessment part I: model development. *JAWRA Journal of the American Water Resources Association* 34 (1), 73–89.
- Bannwarth, M., Hugschmidt, C., Sangchan, W., Lamers, M., Ingwersen, J., Ziegler, A., Streck, T., 2014. Simulation of stream flow components in a mountainous catchment in northern Thailand with SWAT, using the ANSELM calibration approach. *Hydrological Processes* 29 (6), 1340–1352.
- Benaman, J., Shoemaker, C.A., Haith, D.A., 2005. Calibration and validation of soil and water assessment tool on an agricultural watershed in upstate New York. *Journal of Hydrologic Engineering* 10 (5), 363–374.
- Cao, W., Bowden, W.B., Davie, T., Fenemor, A., 2006. Multi-variable and multi-site calibration and validation of SWAT in a large mountainous catchment with high spatial variability. *Hydrological Processes* 20 (5), 1057–1073.
- Chu, T., Shirmohammadi, A., 2004. Evaluation of the SWAT model's hydrology component in the Piedmont physiographic region of Maryland. *Transactions of the ASAE* 47, 1057–1073.
- Dinpashoh, Y., Fakheri-Fard, A., Moghaddam, M., Jahanbakhsh, S., Mirnia, M., 2004. Selection of variables for the purpose of regionalization of Iran's precipitation climate using multivariate methods. *Journal of Hydrology* 297 (1), 109–123.
- Faramarzi, M., Abbaspour, K.C., Schulin, R., Yang, H., 2009. Modelling blue and green water resources availability in Iran. *Hydrological Processes* 23 (3), 486–501.
- Feng, X., Zhang, G., Xu, Y.J., 2013. Simulation of hydrological processes in the Zhalong wetland within a river basin, Northeast China. *Hydrology & Earth System Sciences* 17, 2797–2807.
- Gassman, P.W., Reyes, M.R., Green, C.H., Arnold, J.G., 2007. The soil and water assessment tool: historical development, applications, and future research directions. Center for Agricultural and Rural Development, Iowa State University, 50 (4), 1211–1250.
- Ghobadi, Y., Pradhan, B., Shafri, H.Z., bin Ahmad, N., Kabiri, K., 2015. Spatio-temporal remotely sensed data for analysis of the shrinkage and shifting in the Al Hawizeh wetland. *Environmental Monitoring and Assessment* 187 (1), 1–17.
- Hörmann, G., Köpflin, N., Cai, Q., Fohrer, N., 2009. Using a simple model as a tool to parameterise the SWAT model of the Xiangxi river in China. *Quaternary International* 208, 116–120.

- Huang, Z., Xue, B., Pang, Y., 2009. Simulation on stream flow and nutrient loadings in Gucheng Lake, Low Yangtze River Basin, based on SWAT model. *Quaternary International* 208, 109–115.
- Jacobs, J., Angerer, J., Vitale, J., Srinivasan, R., Kaitho, R., 2007. Mitigating economic damage in Kenya's upper Tana River basin: an application of Arc-View SWAT. *Journal of Spatial Hydrology* 7 (1), 23–46.
- Jayakrishnan, R., Srinivasan, R., Santhi, C., Arnold, J., 2005. Advances in the application of the SWAT model for water resources management. *Hydrological Processes* 19 (3), 749–762.
- Jones, C., Sultan, M., Yan, E., Milewski, A., Hussein, M., Al-Dousari, A., Al-Kaisy, S., Becker, R., 2008. Hydrologic impacts of engineering projects on the Tigris–Euphrates system and its marshlands. *Journal of Hydrology* 353 (1), 59–75.
- Khoi, D.N., Suetsugi, T., 2014. The responses of hydrological processes and sediment yield to land-use and climate change in the Be River Catchment, Vietnam. *Hydrological Processes* 28, 640–652.
- Kim, N., Shin, A., Lee, J., 2010. Effects of streamflow routing schemes on water quality with SWAT. *Transactions of the ASABE* 53 (5), 1457–1468.
- Kousari, M.R., Malekinezhad, H., Ahani, H., Zarch, M.A.A., 2010. Sensitivity analysis and impact quantification of the main factors affecting peak discharge in the SCS curve number method: an analysis of Iranian watersheds. *Quaternary International* 226 (1), 66–74.
- Liu, L., Liu, Z., Ren, X., Fischer, T., Xu, Y., 2011. Hydrological impacts of climate change in the Yellow River Basin for the 21st century using hydrological model and statistical downscaling model. *Quaternary International* 244 (2), 211–220.
- Mango, L., Melesse, A., McClain, M., Gann, D., Setegn, S., 2011. Land use and climate change impacts on the hydrology of the upper Mara River Basin, Kenya: results of a modeling study to support better resource management. *Hydrology & Earth System Sciences* 15 (7), 2245–2258.
- Marjanizadeh, S., Qureshi, A.S., Turrall, H., Talebzadeh, P., 2009. From Mesopotamia to the third millennium: the historical trajectory of water development and use in the Karkheh River Basin, Iran. *IWMI* 51.
- Masih, I., Ahmad, M.-u.-D., Uhlenbrook, S., Turrall, H., Karimi, P., 2009. Analysing streamflow variability and water allocation for sustainable management of water resources in the semi-arid Karkheh river basin, Iran. *Physics and Chemistry of the Earth, Parts A/B/C* 34, 329–340.
- Masih, I., Maskey, S., Uhlenbrook, S., Smakhtin, V., 2011. Impact of upstream changes in rain-fed agriculture on downstream flow in a semi-arid basin. *Agricultural Water Management* 100 (1), 36–45.
- Moriasi, D., Arnold, J., Van Liew, M., Bingner, R., Harmel, R., Veith, T., 2007. Model evaluation guidelines for systematic quantification of accuracy in watershed simulations. *Transactions of the ASABE* 50 (3), 885–900.
- Muthuwatta, L., Bos, M., Rientjes, T., 2010. Assessment of water availability and consumption in the Karkheh River Basin, Iran—Using remote sensing and geostatistics. *Water Resources Management* 24 (3), 459–484.
- Nash, J., Sutcliffe, J., 1970. River flow forecasting through conceptual models part I—A discussion of principles. *Journal of Hydrology* 10 (3), 282–290.
- Neitsch, S., Arnold, J., Kiniry, J., Williams, J., King, K., 2002. *Soil and Water Assessment Tool (Version 2000)—theoretical Documentation*. Texas Water Research Institute, College Station, TX.
- Neitsch, S., Arnold, J., Kiniry, J., Williams, J., King, K., 2005. *Soil and Water Assessment Tool: Theoretical Documentation, Version 2005*. Texas, USA.
- Olivera, F., Valenzuela, M., Srinivasan, R., Choi, J., Cho, H., Koka, S., Agrawal, A., 2006. ARCGIS-SWAT: a geodata model and GIS interface for SWAT1. *JAWRA Journal of the American Water Resources Association* 42 (2), 295–309.
- Santhi, C., Arnold, J.G., Williams, J.R., Dugas, W.A., Srinivasan, R., Hauck, L.M., 2001. Validation of the Swat Model on a Large River Basin with Point and Nonpoint Sources1. Wiley Online Library, pp. 1169–1188.
- Santhi, C., Srinivasan, R., Arnold, J.G., Williams, J., 2006. A modeling approach to evaluate the impacts of water quality management plans implemented in a watershed in Texas. *Environmental Modelling & Software* 21 (8), 1141–1157.
- Schuol, J., Abbaspour, K.C., Srinivasan, R., Yang, H., 2008. Estimation of freshwater availability in the West African sub-continent using the SWAT hydrologic model. *Journal of Hydrology* 352, 30–49.
- Seo, M., Yen, H., Kim, M.-K., Jeong, J., 2014. Transferability of SWAT Models between SWAT2009 and SWAT2012. *Journal of Environmental Quality* 43 (3), 869–880.
- Setegn, S.G., Rayner, D., Melesse, A.M., Dargahi, B., Srinivasan, R., 2011. Impact of climate change on the hydroclimatology of Lake Tana Basin, Ethiopia. *Water Resources Research* 47, 1–13.
- Setegn, S.G., Srinivasan, R., Dargahi, B., 2008. Hydrological modelling in the Lake Tana Basin, Ethiopia using SWAT model. *The Open Hydrology Journal* 2, 49–62.
- Setegn, S.G., Srinivasan, R., Melesse, A.M., Dargahi, B., 2010. SWAT model application and prediction uncertainty analysis in the Lake Tana Basin, Ethiopia. *Hydrological Processes* 24, 357–367.
- Shi, P., Chen, C., Srinivasan, R., Zhang, X., Cai, T., Fang, X., Qu, S., Chen, X., Li, Q., 2011. Evaluating the SWAT model for hydrological modeling in the Xixian watershed and a comparison with the XAJ model. *Water Resources Management* 25 (10), 2595–2612.
- Singh, J., Knapp, H.V., Arnold, J., Demissie, M., 2005. Hydrological modeling of the iroquois river watershed using HSPF and SWAT1. *JAWRA Journal of the American Water Resources Association* 41 (2), 343–360.
- Srinivasan, R., Zhang, X., Arnold, J., 2010. SWAT ungauged: hydrological budget and crop yield predictions in the Upper Mississippi River Basin. *Transactions of the ASABE* 53 (5), 1533–1546.
- Xu, H., Taylor, R.G., Kingston, D.G., Jiang, T., Thompson, J.R., Todd, M.C., 2010. Hydrological modeling of River Xiangxi using SWAT2005: a comparison of model parameterizations using station and gridded meteorological observations. *Quaternary International* 226, 54–59.
- Xu, Z., Zhao, F., Li, J., 2009. Response of streamflow to climate change in the headwater catchment of the Yellow River basin. *Quaternary International* 208, 62–75.
- Yan, B., Fang, N., Zhang, P., Shi, Z., 2013. Impacts of land use change on watershed streamflow and sediment yield: an assessment using hydrologic modelling and partial least squares regression. *Journal of Hydrology* 484, 26–37.
- Yang, J., Reichert, P., Abbaspour, K., Xia, J., Yang, H., 2008. Comparing uncertainty analysis techniques for a SWAT application to the Chaohe Basin in China. *Journal of Hydrology* 358, 1–23.
- Ye, L., Grimm, N.B., 2013. Modelling potential impacts of climate change on water and nitrate export from a mid-sized, semiarid watershed in the US Southwest. *Climatic Change* 120, 419–431.